Biodesign

pISSN 2288-6982 | eISSN 2288-7105

CRYSTALLIZATION P 107-109

Phase determination of a homogentisate dioxygenase from *Comamonas* sp. strain P19

Suk-Youl Park[1], Byoung Yul Soh[2], Jong-Chan Chae[3] and Jeong-Sun Kim[4]*

[1]Pohang Accelerator Laboratory, Pohang University of Science and Technology, 80 Jigokro-127-Beongil, Nam-gu, Pohang, Gyeongbuk 37673, Korea, [2]Department of Biochemistry, College of Medicine, Seonam University, Namwon 55724, Republic of Korea, [3]Division of Biotechnology, Chonbuk National University, Iksan 54596, Republic of Korea, [4]Department of Chemistry, College of Natural Sciences, Chonnam National University, Yongbong-ro 77, Buk-gu, Gwangju 61186, Korea.
*Correspondence: jsunkim@chonnam.ac.kr

In *Comamonas* sp. strain P19, homogentisate 1,2-dioxygenase (HGO) catalyzes the conversion of homogentisate to 4-maleylacetoacetate by aromatic ring scission, in the breakdown of tyrosine and phenylalanine. To determine the molecular background of the enzymatic mechanism of HGO in this zinc-resistant organism, *hmgA* encoding HGO of *Comamonas* sp. strain P19 was cloned, and the expressed protein was purified. The protein was crystallized in solutions I [25% (w/v) polyethylene glycol 3350 and 0.1 M trisodium citrate at pH 5.6] and II [1.4 M ammonium tartrate and 0.1 M bis-Tris at pH 5.5]. X-ray diffraction data were collected to 1.8 Å resolution using synchrotron radiation. The crystal belongs to the orthorhombic space group $P2_12_12_1$, with unit cell dimensions of a = 73.2 Å, b = 100.0 Å, and c = 134.9 Å. A traceable electron density map was calculated using anomalous diffraction data obtained from a crystal soaked in zinc ions.

INTRODUCTION

The degradation of tyrosine and phenylalanine involves the metabolic intermediates fumarate and acetoacetate, which can be converted into glucose or oxidized in the citric acid cycle as a part of cellular respiration. Homogentisate 1,2-dioxygenase (HGO; EC 1.13.11.5) is one of the six enzymes involved in the metabolic pathway of tyrosine and phenylalanine. It catalyzes oxidative opening of the aromatic ring and converts homogentisate (HG) into 4-maleylacetoacetate (Knox & Edwards, 1955b). In mammals, deficiency in homogentisate 1,2-dioxygenase results in alkaptonuria (La Du et al., 1958), a disease characterized by polymerization of the quinone oxidation product of homogentisate, which is known as the ochronotic pigment, and its accumulation in connective tissues (O'Brien et al., 1963), resulting in the development of arthritis (Fernandez-Canon et al., 1996; Rodriguez et al., 2000).

Iron-dependent HGOs utilizing non-heme Fe^{2+} incorporate both atoms of molecular oxygen into homogentisate (Knox & Edwards, 1955a), which cleaves between the C-1 and C-2 carbons substituted with the carboxyl methyl group and hydroxyl group of the aromatic ring in homogentisate (Borowski et al., 2005). The crystal structure of human HGO exhibits an active-site Fe^{2+} coordinated by two histidines and one glutamate to form the facial triad of an iron-binding motif (Titus et al., 2000; Que, 2000; Jeoung et al., 2013). The facial triad motif is found in several non-homologous ferrous-dependent enzymes, especially in extradiol catechol dioxygenase. In the mechanism proposed by Borowski et al., the deprotonated carboxyl and ortho-hydroxyl oxygens of HG replace two water molecules as a bidentate ligand to form an octahedral arrangement of the iron ligand, and subsequently the dioxygen reacts with the aromatic ring to form a peroxo-bridged intermediate at C-1.

A recent time-resolved study of the HG complex structure identified a resting state and three different reaction intermediates, which suggest the subsequent reaction mechanism of oxidative aromatic ring cleavage of HG (Jeoung et al., 2013). In the active site structures of the resting-state HGO, the C2 hydroxyl group of HG is deprotonated with a water molecule, and it then occupies one coordination site, replacing one of two water molecules as a monodentate ligand in the octahedral arrangement of the iron atom. HG is further stabilized

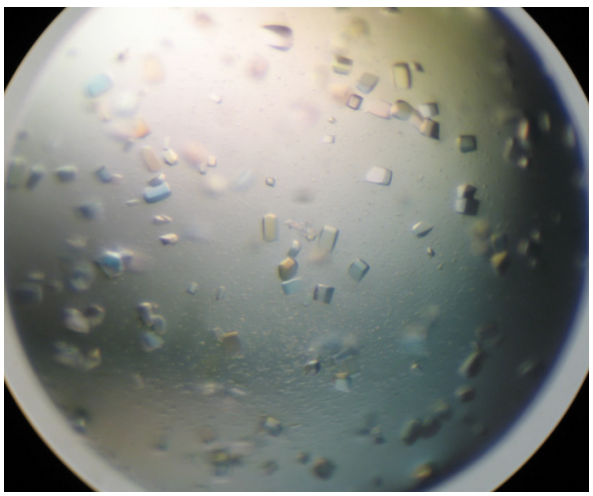

FIGURE 1 | ctHGO crystals grown at 291 K within 3 days with maximum dimensions of approximately 0.05 × 0.05 × 0.05 mm^3.

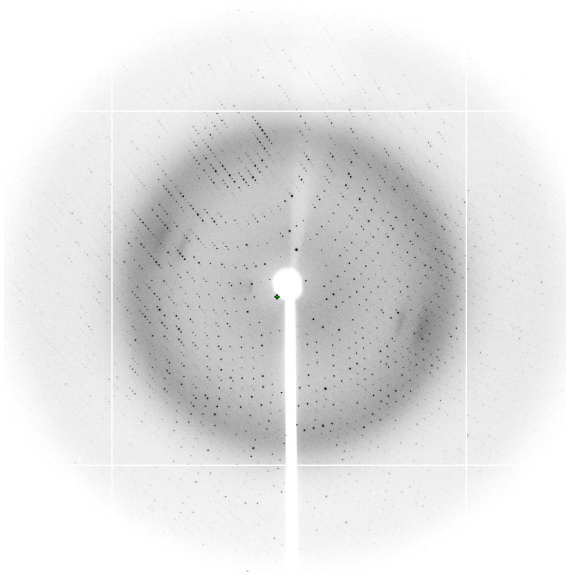

FIGURE 2 | Representative x-ray diffraction image of ctHGO. The crystal was exposed for 10 s over a 1° oscillation range. The edge of the detector corresponds to a resolution of 1.8 Å.

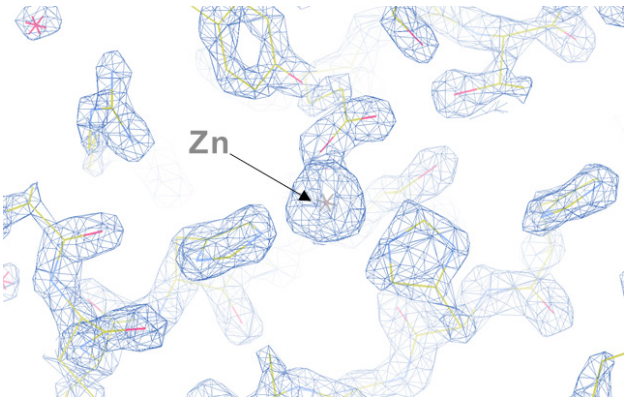

FIGURE 3 | Electron density map at one of the four zinc ion sites. The automatically built residues were drawn using thin stick models in the 2*Fo - Fc* electron-density map contoured at 4.0 σ in the program *Coot*.

by interacting with the C1 carboxyl group and C5 hydroxyl group via histidine and tyrosine, respectively. Then, reduction of the dioxygen generates the peroxo-intermediate with the C-2.

Like human HGO and catechol dioxygenase that has shown ~5% sequence identity, HGO of *Comamonas* sp. strain P19 (ctHGO) has also exhibited a dioxygenase activity with iron ions. However, this enzyme has also shown a glyoxalase activity with divalent metal ions (data not shown). ctHGO is a fairly small protein of 24.7 kDa compared to human HGO of 48.0 kDa and includes a sequence motif that is frequently found in glyoxalase I. Hence it is of high interest to understand how this protein can switch enzyme activities depending on the bound metal ions.

To determine the catalytic mechanism of ctHGO at the molecular level, we cloned, expressed, purified, and crystallized ctHGO. Here, we analyze its X-ray diffraction data and report the phase determination for the first bacterial HGO crystal structure.

RESULTS AND DISCUSSION

Crystals suitable for x-ray diffraction experiments were obtained by the hanging-drop vapor-diffusion method at 291 K within 3 days using two precipitant solutions: solution I [20% (w/v) polyethylene glycol 3350, 0.3 M ammonium acetate and 0.1 sodium citrate at pH 7.5] and solution II [1.4 M ammonium tartrate and 0.1 M bis-Tris at pH 5.5]. From solution II, the dimensions of the crystal used for the diffraction experiments were approximately 0.05 x 0.05 x 0.05 mm^3 (Figure 1) and the crystal diffracted to 1.8 Å resolution (Figure 2). For subsequent structural determination using the molecular replacement method, a primary sequence homology search of the Protein Data Bank failed to find suitable structural homologues, although the sequence homologies exceeded 30%. Therefore, to obtain phasing information, single-wavelength anomalous dispersion data of the zinc-soaked crystal produced in

TABLE 1 | Data collection and processing for ctHGO

Parameters	High resolution	Zn-Peak
Synchrotron	BL17U, SSRF	BL17U, SSRF
Wavelength (Å)	1.00	1.28
Space group	$P2_12_12_1$	$P2_12_12_1$
Cell parameters	a = 73.2, b = 100.0, c = 134.9	a = 73.2, b = 100.4, c = 135.8
Resolution (Å)	50.0 - 1.80 (1.86 - 1.80)	50.0–2.50 (2.59-2.50)
Completeness (%)	90.6 (72.0)	99.6 (97.5)
R_{merge} [a] (%)	8.0 (30.8)	10.8 (41.7)
Reflections, Total/Unique	348,852/83,060	213,007/34,356
Multiplicity	4.2	6.2
Temperature (K)	100	100
I/Sigma[b] (*I*)	18.7 (2.0)	23.8 (3.1)
FOM[c], Solve/Resolve (50-2.8 Å)		0.19/0.67

Values in parentheses are for the highest-resolution shell. FOM, figure of merit. [a]$R_{merge} = \sum_{hkl}[\sum_i (|I_{hkl,i} - \langle I_{hkl}\rangle|)]/\sum_{hkl,i} \langle I_{hkl}\rangle$, where $I_{hkl,i}$ is the intensity of an individual measurement of the reflection with Miller indices *hkl* and $\langle I_{hkl}\rangle$ is the mean intensity of that reflection. [b]I/Sigma means <*I*>/<Sigma>. [c]Figure of merit = $|\sum P(\alpha)e^{i\alpha}/\sum P(\alpha)|$, where $P(\alpha)$ is the phase probability distribution and is the phase (50.0 - 2.8 Å).

solution I were collected at 1.28257 Å. The zinc-soaked crystals belong to the orthorhombic space group P212121, with the following unit-cell parameters: a = 73.2 Å, b = 100.4 Å, and c = 135.8 Å. Four zinc atoms in the asymmetric unit (Figure 3) were identified at 2.8 Å resolution using the program SOLVE (Terwilliger, 2003). The electron density was improved by density modification using the programs RESOLVE (Terwilliger, 2003) and PHENIX (Adams et al., 2010), resulting in 30% of the modeled residues being built automatically. Crystallographic model building and refinement of the structure to 1.8 Å resolution are in progress.

METHODS

Cloning, expression and purification of ctHGO

The *hmgA* gene encoding ctHGO (W6AP65; Met1-Lys216) was amplified from *Comamonas* sp. strain P19 chromosomal DNA by polymerase chain reaction (PCR) using the forward primer 5'-GGA TCC GAT GAG CCA AGC CGC CCC TAC-3' and the reverse primer 5'-AAG CTT GGG CTT ACC AGG AAC AAA CTC CGG C-3', which contain *Bam*HI and *Hin*dIII recognition sequences (underlined), respectively. The PCR product was ligated into pGEM T-Easy vector (Promega, Madison, Wisconsin, USA). To generate an expression construct, the *hmgA* gene was sequenced and cloned into pET-21b (Novagen, Madison, Wisconsin, USA), resulting in a fusion protein with six histidine residues at the C-terminus.

The expression construct was transformed into *E. coli* strain XL-blue, which was grown in 500 mL LB medium containing ampicillin (100 μg mL^{-1}) at 310 K. After induction by addition of 0.1 mM isopropyl β-D-1-thiogalacto-pyranoside, the culture medium was maintained for a further 5 h at 310 K. Cells were harvested by centrifugation at 6000 rpm and 277 K for 20 min.

The cell pellet was lysed by ultrasonication in ice-cold buffer (50 mM NaH_2PO_4, pH 8.0, 300 mM NaCl, 10 mM imidazole) supplemented with 100 mg mL^{-1} lysozyme. Cell debris was removed by centrifugation at 12,000 rpm for 20 min. ctHGO was purified using IDA Excellose chelating resin (Bioprogen, Daejeon, Korea). The resin was rinsed extensively with washing buffer (50 mM NaH_2PO_4, pH 8.0, 300 mM NaCl, 20 mM imidazole), and the bound protein was eluted using elution buffer (50 mM NaH_2PO_4, pH 8.0, 300 mM NaCl, 250 mM imidazole). The resulting protein was > 95% pure according to SDS-PAGE and Coomassie Blue staining. ctHGO contained 13 extra residues (KLAAALEHHHHHH) at the C-terminus.

Crystallization

For crystallization, the purified ctHGO protein was concentrated to 10 mg/mL in a buffer consisting of 20 mM Tris-HCl at pH 7.5 and 300 mM NaCl. The protein concentration was determined using an extinction coefficient of 1.215 mg mL^{-1} cm^{-1} at 280 nm, which was calculated from its amino acid sequence. Initial crystallization screening of ctHGO was performed using Sparse Matrix Screening (Jancarik & Kim, 1991) from Hampton Research and Emerald BioSystems using a sitting-drop vapor-diffusion method. In the initial crystallization screening experiments, 0.5 mL protein solution was mixed with 0.5 mL reservoir solution and equilibrated against 50 mL reservoir solution. Initial crystals were obtained under two conditions: 1) 25% (w/v) polyethylene glycol 3350, 0.2 M ammonium acetate, sodium citrate at pH 7.5, and 2) 1.1 M ammonium tartrate dibasic at pH 7.0. To obtain crystals suitable for x-ray diffraction, the precipitant and protein concentrations, buffer pH, and temperature were changed systematically, and various equilibrium strategies were evaluated, such as the hanging-drop and sitting-drop vapor-diffusion methods.

X-ray diffraction data collection

For the diffraction experiments, crystals were briefly immersed in a precipitant solution containing 20% (v/v) glycerol as a cryoprotectant and were immediately placed in a 100 K nitrogen-gas stream. Native x-ray diffraction data were collected at BL17U, in the Shanghai Synchrotron Radiation Facility (SSRF, Shanghai, China), using 1° oscillation per image at a crystal-to-detector distance of 200 mm. The crystal was exposed for 10 s per image. A dataset was collected to 1.8 Å resolution from a single crystal. The data were indexed and scaled using HKL-2000 software (Otwinowski & Minor, 1997). The data-collection statistics are summarized in Table 1.

CONFLICT OF INTEREST

The authors declare that there is no conflict of interest.

ACKNOWLEDGEMENTS

This work was funded by Chonnam National University (Project Administration No. 2015-0597).

Original Submission: Aug 24, 2017
Revised Version Received: Sep 11, 2017
Accepted: Sep 16, 2017

REFERENCES

Adams, P.D., Afonine, P.V., Bunkoczi, G., Chen, V.B., Davis, I.W., Echols, N., Headd, J.J., Hung, L.W., Kapral, G.J., Grosse-Kunstleve, R.W., McCoy, A.J., Moriarty, N.W., Oeffner, R., Read, R.J., Richardson, D.C., et al. (2010). PHENIX: a comprehensive Python-based system for macromolecular structure solution. *Acta Crystallogr D Biol Crystallogr* **66**, 213-221.

Borowski, T., Georgiev, V., and Siegbahn, P.E. (2005). Catalytic reaction mechanism of homogentisate dioxygenase: a hybrid DFT study. *J Am Chem Soc* **127**, 17303-17314.

Fernandez-Canon, J.M., Granadino, B., Beltran-Valero de Bernabe, D., Renedo, M., Fernandez-Ruiz, E., Penalva, M.A., and Rodriguez de Cordoba, S. (1996). The molecular basis of alkaptonuria. *Nat Genet* **14**, 19-24.

Jeoung, J.H., Bommer, M., Lin, T.Y., and Dobbek, H. (2013). Visualizing the substrate-, superoxo-, alkylperoxo-, and product-bound states at the nonheme Fe(II) site of homogentisate dioxygenase. *Proc Natl Acad Sci U S A* **110**, 12625-12630.

Knox, W.E., and Edwards, S.W. (1955a). Homogentisate oxidase of liver. *J Biol Chem* **216**, 479-487.

Knox, W.E., and Edwards, S.W. (1955b). The properties of maleylacetoacetate, the initial product of homogentisate oxidation in liver. *J Biol Chem* **216**, 489-498.

La Du, B.N., Zannoni, V.G., Laster, L., and Seegmiller, J.E. (1958). The nature of the defect in tyrosine metabolism in alcaptonuria. *J Biol Chem* **230**, 251-260.

O'Brien, W.M., La Du, B.N., and Bunim, J.J. (1963). Biochemical, pathologic and clinical aspects of alcaptonuria, ochronosis and ochronotic arthropathy. *Am J Med* **34**, 813-838.

Otwinowski, Z., and Minor, W. (1997). Processing of X-ray diffraction data collected in oscillation mode. *Methods Enzymol* **276**, 307-326.

Que, L., Jr. (2000). One motif--many different reactions. *Nat Struct Biol* **7**, 182-184.

Rodriguez, J.M., Timm, D.E., Titus, G.P., Beltran-Valero De Bernabe, D., Criado, O., Mueller, H.A., Rodriguez De Cordoba, S., and Penalva, M.A. (2000). Structural and functional analysis of mutations in alkaptonuria. *Hum Mol Genet* **9**, 2341-2350.

Terwilliger, T.C. (2003). SOLVE and RESOLVE: automated structure solution and density modification. *Methods Enzymol* **374**, 22-37.

Titus, G.P., Mueller, H.A., Burgner, J., Rodriguez De Cordoba, S., Penalva, M.A., and Timm, D.E. (2000). Crystal structure of human homogentisate dioxygenase. *Nat Struct Biol* **7**, 542-546.

